

## **UC Merced**

### **Other Recent Work**

#### **Title**

Effects of heat treatment and cooling on the mechanical properties of 3D Printed Poly(Lactic Acid)

#### **Permalink**

<https://escholarship.org/uc/item/2t50w1qw>

#### **Author**

Johnson, James Orin

#### **Publication Date**

2022-04-01

# Effects of heat treatment and cooling on the mechanical properties of 3D Printed Poly(Lactic Acid)

MSE 112  
Rod Villa, James Johnson  
May 2022

## **Abstract:**

In metallurgy it is well known that heat treatment can change the properties of a material, however the general populace is unaware that plastics can also be heat treated for tunable properties. The effects of annealing poly(lactic acid) (PLA) is reported to increase its strength versus untreated PLA samples of similar geometry<sup>1</sup>. This study uses tensile and bending tests to investigate the change in mechanical properties that PLA samples can achieve due to heat treatment and cooling. This study found that PLA increased in bending strength 16% when compared to the non-treated samples. Both heat-treated samples were more brittle in the tensile test, and the optical micrographs show the fractures in the heat-treated samples were smooth characteristic of crack propagation with minimal craze formation, and rough for the non-treated samples suggesting that crazes were absorbing much greater fracture energy than the heat-treated samples.

## **Intro:**

PLA is popular for use as a material for biomedical<sup>2</sup>, prototyping<sup>3</sup> and disposable<sup>4</sup> applications due to its ability to biodegrade, as it can fully break down into lactide<sup>5</sup>. 3-D printing is a popular prototyping solution because it allows for the fabrication of high detail, low-cost prototypes with unique geometries. However, it has limitations, particularly due to the nature of additive manufacturing processes like 3-D printing.

Additive manufacturing is the process by which material is laid out in a plane, with cross sections added layer by layer until a complete object is formed. It is a time-consuming process to economically produce hundreds of units of a thermoplastic component or product (Figure 1)<sup>6</sup>. This layer-by-layer approach has consequences aside from the slow print time, in that the bonds between each layer are particularly weaker than a similarly injected molded sample<sup>7</sup>.

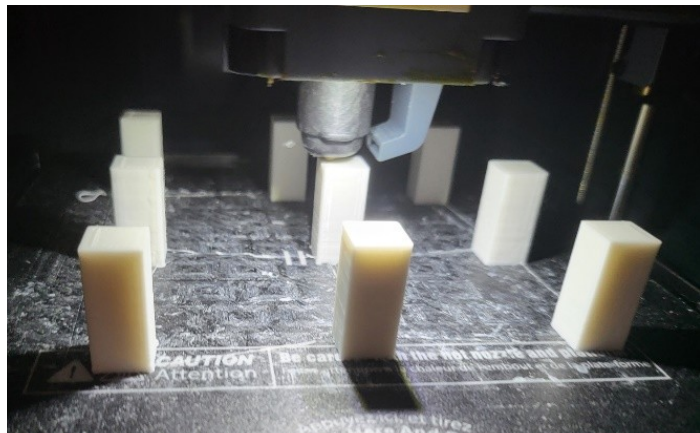


Figure 1: PLA samples being printed one layer at a time using a Monoprice Voxel 3D Printer.

In the 3-D printing community, a method to improve the durability and glass transition temperature of models printed of PLA is to anneal them post-print<sup>1</sup> as this will increase the degree of crystallinity of the material<sup>8</sup>. An investigation of the effects caused by annealing is studied in this paper and

examined through tensile and bending tests, in addition to optical microscopy. PLA's glass transition temperature is typically between 55 to 60 °C<sup>9</sup> therefore it is reasonable to conclude that if annealed above the glass temperature range, the layers from the printing process can refine and strengthen the specimen.

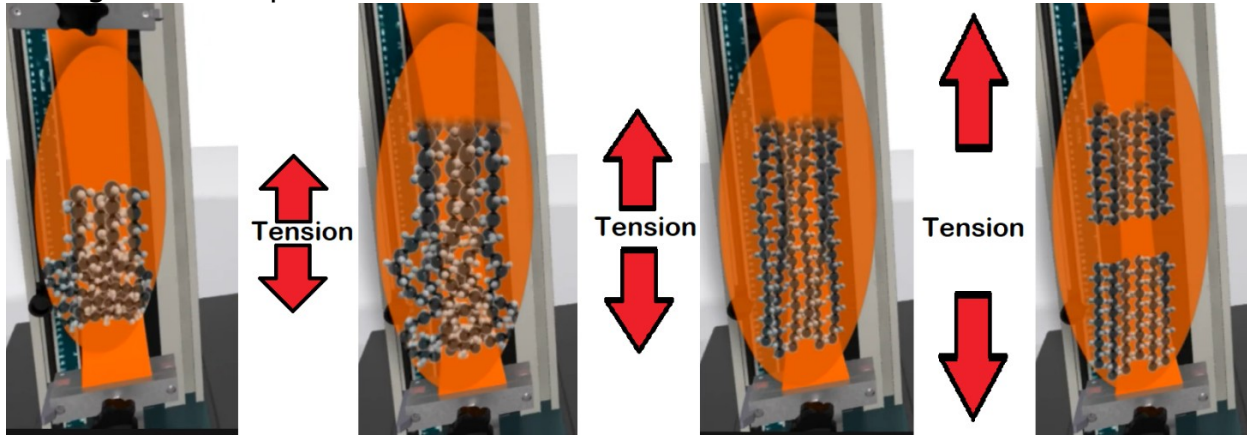


Figure 2: Tensile deformation of polymer samples (credit: Tinius Olsen<sup>10</sup>)

Tensile tests were performed in this study to assess the change in tensile strength from the increased crystallinity within the material due to the annealing process. Polymer samples, such as PLA, undergo a different mechanism under tensile strain than metals in that strain will cause an alignment of polymer chains during necking as shown in figure 2<sup>10</sup>. Additionally, thermoplastics like PLA may experience crazing, in which microvoids form and propagate perpendicular to the applied tensile stress which occur at highly stressed regions. PLA in particular has been reported to undergo massive crazing<sup>11</sup>.

When an object is acted upon by a force, it develops stress ' $\sigma$ ' which is represented as a function of the applied load ' $F$ ' over the original cross-sectional area ' $A_o$ ' of the object's geometry before a load was applied as shown in equation 1. Strain ' $\epsilon$ ' is derived using the change of length ' $\Delta l$ ' from the original length ' $l_o$ ' of the sample (equation 2).

$$\sigma = \frac{F}{A_o} \quad (\text{eq. 1}) \quad \& \quad \epsilon = \frac{\Delta l}{l_o} \quad (\text{eq. 2})$$

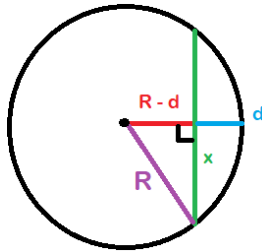
Bending tests were utilized to observe any changes in the flexural strength of the sample and to gauge if the bonds between individual layers from the printing process became stronger due to annealing above the glass transition temperature. The maximum bending moment ' $M$ ' was determined as a function of the load ' $F$ ' and the distance ' $x$ ' from one supported end of the sample to the other as shown in equation 3 and was used to determine the flexural stress applied by multiplying it by the distance from the center of

the specimen to the surface 'c', all over the moment of inertia of the cross section 'I' as represented in equation 4.

$$M = \frac{F \cdot x}{4} \quad (\text{eq. 3}) \quad \& \quad \sigma = \frac{Mc}{I} \quad (\text{eq. 4})$$

To determine the strain due to bending, the deflection measurement along with the known chord length of the bending test was determined using Pythagorean's theorem reduced into equation 5 to determine the radius of curvature 'R' where 'd' is the deflection using the trigonometry represented in figure 3.

$$R^2 = (R-d)^2 + \left(\frac{x}{2}\right)^2 \rightarrow R = \frac{x^2}{8d} + \frac{d}{2} \quad (\text{eq. 5})$$



The strain due to bending was calculated as a function of radius of curvature and the distance to the surface of the sample 'c' from its neutral axis as represented in equation 6.

$$\epsilon = \frac{c}{R} \quad (\text{eq. 6})$$

Figure 3:  
Trigonometry to  
determine radius  
of curvature for  
bent samples

The fractures caused by these tests were magnified and imaged via optical microscopy to understand how failure occurred and if the mode of failure for the samples changed as a result of heat treatment.

### Procedures:

The samples were printed from PLA with 100% fill density using a Monoprice Voxel 3D Printer which has an enclosed sample bed that limits possible contamination from the environment during the printing process. The header used for extrusion reached 210°C and the samples were printed at 40 mm per second. The samples were rectangular beams and had a cross sectional area of 5 mm x 5 mm with a height of 120 mm.

Heat-treatment consisted of holding the PLA samples at 100°C isothermally for twenty-four hours inside of aluminum containers (Figure 4). 100°C was chosen as the annealing temperature based off other investigations into ideal annealing temperatures for PLA<sup>12</sup>. Half of the test samples were then quenched in 0°C MiliQ water for rapid



Figure 4: PLA samples: the control samples (left) versus the rapidly cooled (center) and slow cooled (right) heat-treated samples

cooling whereas the other half were allowed to slowly cool in the oven to room temperature.



Figure 5: INSTRON 3369 universal testing machine equipped for tensile testing

The INSTRON 3369 (Figure 5), a universal testing machine, was used for the tensile test and its parameters were controlled via a computer using the software Bluehill 3. To perform this test the sample's dimensions were chosen to fit within the clamps of the device that had a sample width limit of 0.6mm. The clamps were manually set a specific distance apart and returned to the same position once each run of the experiment concluded to allow loading of new samples. The computer program was set to perform tensile testing with a strain rate of 0.25 millimeters per minute.

To load a sample into the device, both clamps needed to be opened to allow the sample to be loaded. Both ends of the sample should have equivalent lengths of the material within each clamp before securing the sample from moving during the experiment. The program had the function to zero-out the universal testing machine's loading and length measurements which ensured that each sample tested would share the same origin. Once the program ran, the sample was stretched manually halted once the break occurred.

The first sample tested was the control sample. The data was saved, and the program was reset for the next sample in which the steps were repeated. The second sample to be tested was the heat-treated, slow cooled sample, and the third sample was the rapid cooled sample. Once all the data was collected for the samples, it was transferred to an Excel document for analysis and used to calculate stress and strain values. Samples were labeled and set aside for further observation under the optical microscope.

The INSTRON 3369 universal testing machine was also used for bending tests. The clamps were both completely removed from the machine and replaced by the bar cross section on the top only, as seen in Figure 6, such that a three-point bending test could be performed. A custom stand was used as a support as the machine's included supports had a minimum length requirement of 150 millimeters. The materials used for this support were punctured steel bars, Zinc bolt and nuts, and four wooden legs, all of which were chosen for having a much higher strength than PLA, to minimize

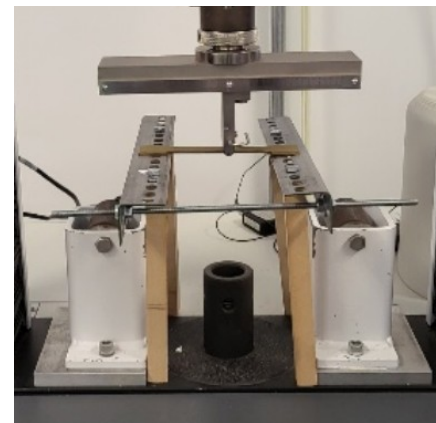


Figure 6: Bending test configuration for the INSTRON 3369 with a custom stand for three-point bending

artifacts from stresses applied to these materials as a result of the three-point bending test.

Just before the experiment began, the bar was manually lowered until near contact with the sample and the machine zeroed out for distance and force with the strain rate set to 0.5 millimeters per minute. Similar to the tensile test, the program was then used to run the experiment until fracture in which the device was manually stopped and reset to the starting position and the process repeated for each sample. After the testing was complete the stand was removed, samples were labeled and set aside for further observation under the optical microscope, and the resulting data was transferred to an Excel document for analysis.

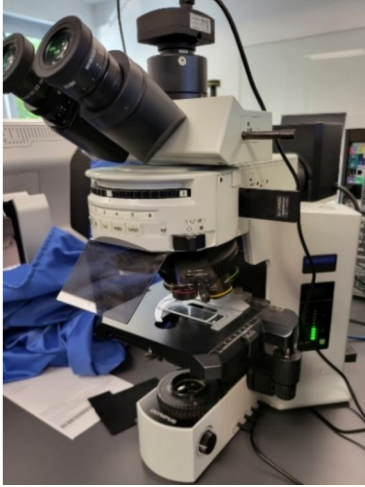


Figure 7: an Olympus BX51 optical microscope, with variable magnifying lenses and reflected light

Using an Olympus BX51 optical microscope (Figure 7), the cracks and fractured surfaces resulting from the universal testing machine were analyzed. Operation of the microscope, as per the user manual<sup>13</sup>, requires that the dust cover be removed prior to use. Reflected light microscopy was used with magnification set to five times, and a slide placed on the stage to hold the samples under observation. The microscope was adjusted using both manually and via the computer. Each sample was focused using the focus adjustment knobs and the stand adjustment dials then refocused for the computer to obtain a clear image of the fractures. The process was repeated for the remaining samples, and once the images were taken, we obtained an image of a calibration slide's scalebar. The data was then manipulated using the software ImageJ for proper scaling of each image with the scalebar.

## **Results:**

Tensile testing collects data that requires a conversion of the load into tensile stress and elongation into strain such that stress/strain curves were generated which allows for identification of the material's properties itself rather than the load applied for the specific geometry of our material. Our control sample proved to have the greatest ultimate tensile strength and did not fail until 26.0 MPa of stress had been applied (Figure 8). Using equation 1, the force at which this occurred was about 650 N. Comparatively, both heat-treated samples had dramatically lower ultimate tensile strength. The quenched sample had the weakest strength whereas the slowly cooled sample was able to maintain most of its strength. The numerical values of

the ultimate tensile strength, the strain at which failure occurred are tabulated in table 1.

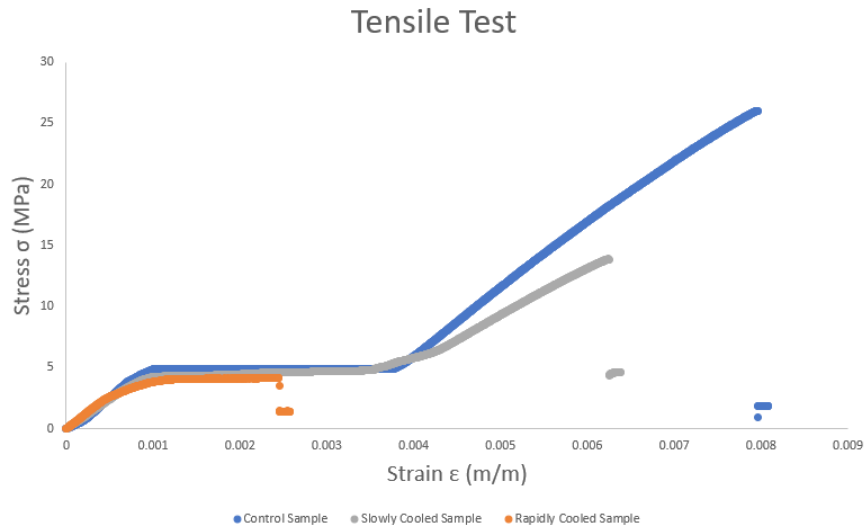


Figure 8: Stress strain plot for tensile testing of poly(lactic acid) 3D printed samples.

Table 1: Tensile Test Results for 0.25mm/min strain rate		
<u>Sample</u>	<u>Ultimate Stress <math>\sigma_{max}</math> (MPa)</u>	<u>Failure Strain <math>\epsilon_{fail}</math> (m/m)</u>
Control	26.0	0.00795
Rapidly Cooled	4.19	0.00244
Slowly Cooled	13.9	0.00624

The tensile force was applied in the same axis that the layers were built upon each other, so these results may indicate that the polymer chains began to arrange in a more ordered fashion, however from Figure 2 we know that tensile strain will cause the polymer chains to align during necking just before failure, thus we believe the alignment of polymer chains occurred during the heat treatment process which allowed for early tensile failure of our samples.

The bending tests' results, in which a normal load is applied to our sample, indicated that the samples had high strength when being bent compared to an untreated sample versus tensile testing that decreased in strength when annealed. It is important to note that for this reported data, the extension may be off by a factor of 0.02 mm as a correction was performed to eliminate extension data prior to the sample experiencing a load from the testing device. Table 3 showcases not only the deflection but



also the flexural stress, strain and maximum bending moment derived using equations 3, 4 and 6.

The results agree with other investigations<sup>14</sup> that have reached 16.2% increased strength in PLA samples via heat-treatment and shows that the cooling rate is significant when it comes to improving 3D printed samples made from PLA as reported by others<sup>15</sup>. It is interesting that while the max load required to make each heat-treated sample fail were similar, the amount of deflection before failure varied depending on whether the sample was quenched or allowed to slowly cool, with the rapidly cooled samples remaining most flexible.

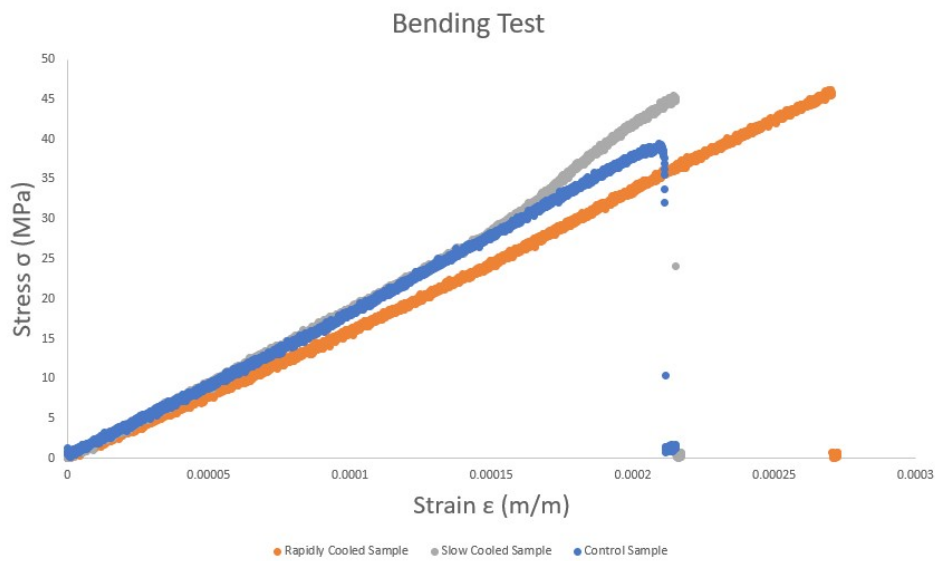


Figure 9: Stress strain plot for bending tests of poly(lactic acid) 3D printed samples

Table 2: Bending Test Results for 0.5mm/min extension rate					
<i>Samples</i>	<i>Max Deflection (mm)</i>	<i>Flexural Stress <math>\sigma_{fs}</math> (MPa)</i>	<i>Strain <math>\epsilon</math> (m/m)</i>	<i>Max Bending Moment (N·m)</i>	<i><math>\sigma_{fs}</math> % increase</i>
Control	2.50	38.8	0.000210	0.808	0
Rapidly Cooled	3.22	46.1	0.000270	0.961	18.8
Slowly Cooled	2.56	45.0	0.000215	0.938	16.0

Observing the samples under optical microscopy the layers in which the sample was printed are clearly visible. Figure 10A, the control sample that underwent the tensile testing had non-uniform edges at its fracture that ran across over multiple print layers. The non-uniform edges indicate a large amount of possible crazing despite the print layers being weak points to the structure implying that the sample's stresses were spread over a great area throughout the material.

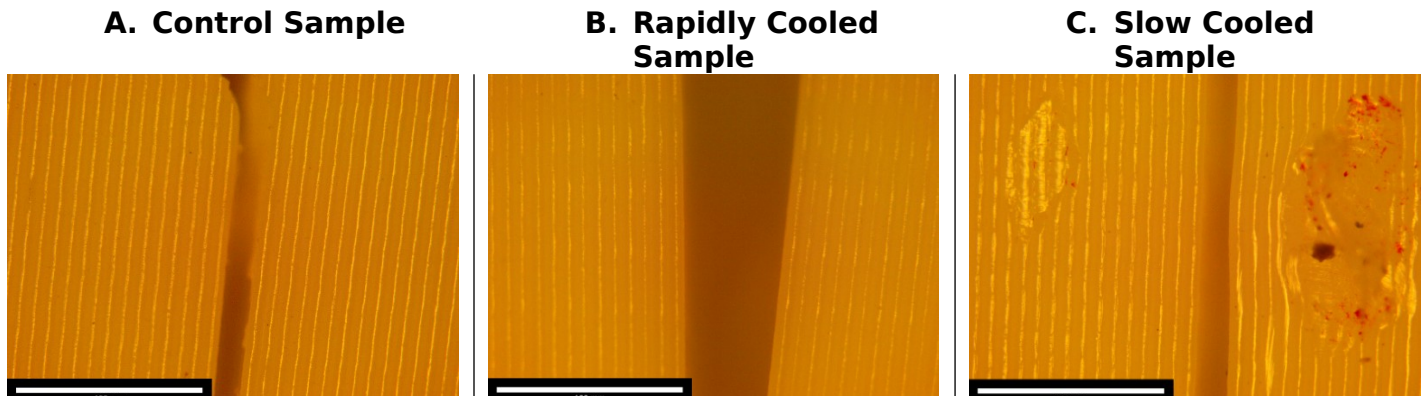


Figure 10: Optical Microscopy analysis of tensile test fractures of each sample; the white scale bar represents 100  $\mu$ m

In contrast to the non-heat-treated sample, the rapidly cooled sample, broken by tensile forces in figure 10B, had a clean separation of print layers. This implies that the sample experienced concentrated localized stresses between layers of the print and that a crack formed along weakest layers. We assume that because crazes were not formed, not enough stress could be absorbed by their formation leading to the early failure of the quenched sample.

The slowly cooled sample, broken by tensile force in figure 10C, gave a unique result in that the fracture was clean, but with layer deformation and a rupture occurring multiple layers away from the fracture point. This suggests that the stresses due to the tensile tests were more widely spread throughout the material compared to the control and quenched samples and that multiple modes of failure were occurring, both crazing and crack propagation through the weak layer however the clean cut suggests the weakest mode of failure was between print layers. The multiple modes of failure, but with less crazing events to absorb stress than the control sample, seems to explain why the slowly cooled sample failed at greater stresses than the rapidly cooled one, but not as much as the control sample.

Bending test results for the non-heat-treated sample, shown in figure 11A, show damage throughout the sample, with ruptures propagating through multiple layers before failure suggesting massive amounts of crazing

occurred. When comparing the bending test data to tensile test data and considering that the fracture did not manage to split the material entirely suggests each layer must have higher compressive strength but weak tensile strength as the failure is similar to that seen in figure 10A. The material failed 'cutting' through a layer, but most of the failure seems to have occurred when a crack propagated completely through a weak layer.

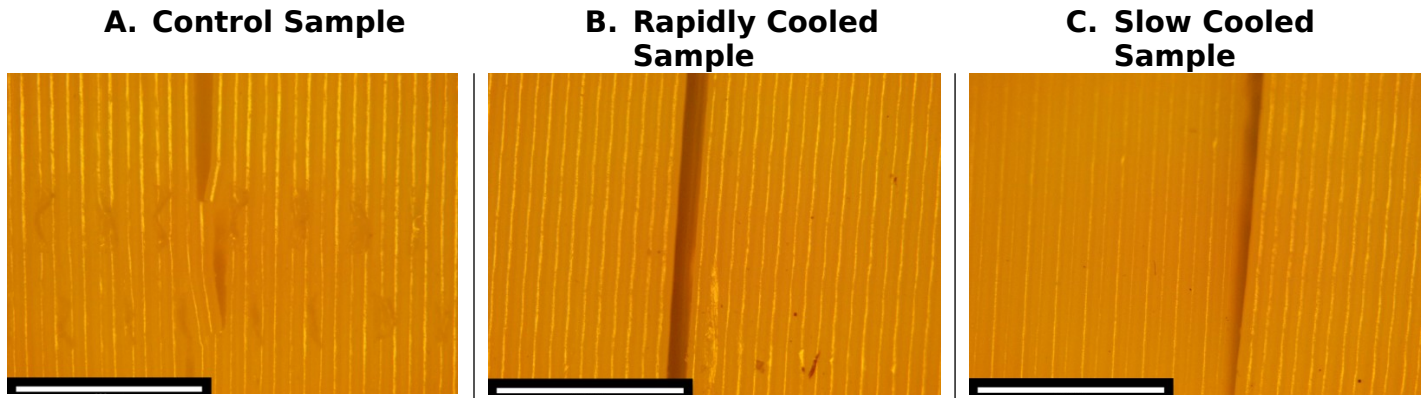


Figure 11: Optical Microscopy analysis of bending test fractures of each sample; the white scale bar represents 100  $\mu$ m

The rapidly cooled sample broke along a single layer with minimal warping of the layers, as can be seen in figure 11B which is similar to what was observed in the rapidly cooled tensile test. This agrees with the earlier assumption that rapid cooling causes material to experience only localized stresses with minimized crazing, where crack propagation between print layers becomes the weakest mode of failure. Unlike the tensile tests however, the material underwent the largest deflection, bending 25% more than the other samples which implies the same assumption as the tensile test in that the polymer chains became more aligned through this process increasing its bendability. The sample broke violently and separated quickly as the excess stress energy must've been released when the polymer chains finally broke.

The slowly cooled sample (figure 11C) had a clean fracture between the print layers; however, it was able to hold a similar amount of load as the rapidly cooled sample, implying that the bonding strength through the entire material was increased. The mode of failure occurring between the print layers shows that stresses were localized in the bending test with no sign of crazing, which was vastly different than the tensile test results, but demonstrates that allowing the material to slow cool maintains rigidity.

### **Conclusion:**

The heat-treatment of PLA can vastly improve the structural integrity of 3D printed objects with control of the cooling rate being critical to the tunability of its properties. Quenching the samples to 0°C showed vastly inferior tensile strength, but superior flexural strength of nearly 19% improvement with 28% greater deflection compared to an untreated sample. Allowing samples enough time to return to room temperature inside the oven partially relaxed the polymer chains maintaining some resistance to tensile strength but highly increased its flexural strength by 16% and maintained its rigidity as it deflected near identically to the control sample. Failure for each

sample was affected by both the heating and cooling processes as well, with rapid cooling causing failure to occur cleanly between layers and slow cooling having different effects on the mode of failure depending on how the load is applied. The ability to tune the stiffness of PLA is useful as it allows for a greater variety in applications of 3D printing, permitting the design of flexible or more durable objects. A more thorough conclusion would include collecting more data and further characterization of 3D printed PLA samples. If given the opportunity of future research into this topic an SEM analysis would be performed to glimpse the surface morphology of fractures to determine whether the proposed mechanics, we suggest are truly occurring. Furthermore, we would like to increase our sample sizes to create more statistically relevant results and conclusions.

## Works Cited:

1. Koci, Jacob. "How to Improve Your 3D Prints with Annealing - Original Prusa 3D Printers." *Original Prusa 3D Printers*, blog.prusa3d.com, 6 Dec. 2019, [https://blog.prusa3d.com/how-to-improve-your-3d-prints-with-annealing\\_31088/](https://blog.prusa3d.com/how-to-improve-your-3d-prints-with-annealing_31088/).
2. *Poly-Lactic Acid Synthesis for Application in Biomedical Devices — A Review*. www.sciencedirect.com, 6 July 2011, <https://doi.org/https://doi.org/10.1016/j.biotechadv.2011.06.019>.
3. Firstpart. "Simple Design Guides for 3D Prototyping with PLA ." *Blogs* □ - *First Part China Limited*, www.firstpart.com, 31 Mar. 2022, [https://www.firstpart.com/news/News\\_Blog/Simple\\_Design\\_Guides\\_for\\_3D\\_Prototyping\\_with\\_PLA.html](https://www.firstpart.com/news/News_Blog/Simple_Design_Guides_for_3D_Prototyping_with_PLA.html).
4. "Bioplastic Cups | Bio Futura - Sustainable Disposables." *Bioplastic Cups | Bio Futura - Sustainable Disposables*, www.biofutura.com, <https://www.biofutura.com/en/disposable-cups/bio-plastic-cups>. Accessed 8 May 2022.
5. Chien, Yi-Chi. *Combustion Kinetics and Emission Characteristics of Polycyclic Aromatic Hydrocarbons from Polylactic Acid Combustion*. www.tandfonline.com, 24 0 2012, <https://doi.org/https://doi.org/10.3155/1047-3289.60.7.849>.
6. Ashby, Michael F. *Materials Selection in Mechanical Design*. Butterworth-Heinemann, 2010.
7. Dawoud, Michael. *Mechanical Behaviour of ABS: An Experimental Study Using FDM and Injection Moulding Techniques*. www.sciencedirect.com, 9 Dec. 2015, <https://doi.org/10.1016/j.jmapro.2015.11.002>.
8. Wach, Radoslaw. *Enhancement of Mechanical Properties of FDM-PLA Parts via Thermal Annealing*. Wiley Online Library, 11 0 2018, <https://doi.org/https://doi.org/10.1002/mame.201800169>.
9. O'Connell, Jackson. *Glass Transition Temperatures of PLA & PETG*. 9 0 2021, <https://doi.org/https://doi.org/10.1002/mame.201800169>.
10. Olsen, Tinius. "Changes to Polymer Chain Arrangement during a Tensile Test (Tinius Olsen 5ST)." *YouTube*, www.youtube.com, 26 Mar. 2015, <https://www.youtube.com/watch?v=-HWeonz8HNE>.
11. Razavi, Masoud. "Crazing and Yielding in Glassy Polymers of High Molecular Weight." *Crazing and Yielding in Glassy Polymers of High Molecular Weight - ScienceDirect*, www.sciencedirect.com, 22 Apr. 2020, <https://www.sciencedirect.com/science/article/pii/S0032386120302809>.
12. Carolo, Lucas. "Annealing PLA for Stronger 3D Prints: 2 Easy Ways." *All3DP*, 6 0 2021, <https://all3dp.com/2/annealing-pla-prints-for-strength-easy-ways/>.

13. *Olympus BX51 Manual*. [https://arf.berkeley.edu/files/webfiles/all/arf/equipment/laboratory/microscope/oly\\_bx51/olympus\\_bx-51\\_bx52\\_microscope\\_manual.pdf](https://arf.berkeley.edu/files/webfiles/all/arf/equipment/laboratory/microscope/oly_bx51/olympus_bx-51_bx52_microscope_manual.pdf). Accessed 8 May 2022.
14. “Better Performing 3D Prints with Annealing, but... - Part 1: PLA &mdash; CNC Kitchen.” *CNC Kitchen*, [www.cnckitchen.com](http://www.cnckitchen.com), 25 Sept. 2019, <https://www.cnckitchen.com/blog/better-performing-3d-prints-with-annealing-but-part-1-pla>.
15. “How to Anneal Your 3D Prints for Strength - 3DSourced.” *3DSourced*, [www.3dsourced.com](http://www.3dsourced.com), 20 Apr. 2022, <https://www.3dsourced.com/rigid-ink/how-to-anneal-your-3d-prints-for-strength/>.